Accepted for Presentation to the IEEE MTT-S Microwave Conference 1998

SPACE ADAPTIVE ANALYSIS OF EVANESCENT WAVEGUIDE FILTERS

Emmanouil M. Tentzeris, Linda P.B. Katehi
Radiation Laboratory, Department of Electrical Engineering and Computer Science
University of Michigan, Ann Arbor, MI 48109–2122, U.S.A.

Abstract- The MRTD scheme is applied to the analysis of evanescent waveguide filters. Specifically, a space adaptive algorithm in 3 dimensions is implemented by thesholding the wavelet values. The results are compared to those obtained by use of the conventional FDTD to indicate considerable savings in memory and computational time.

I Introduction

The Space Adaptive Gridding [1], based on the application of the Multiresolution Analysis principles to the discretization of the time-domain Maxwell's equations [2, 3], has been employed in the analysis of linear and nonlinear structures. It has offered significant savings in memory and execution time requirements. The application of the wavelets improve the conditioning of the simulating algorithm and allow for a space adaptive grid by thresholding the wavelet coefficients. This adaptivity is useful especially in evanescent mode structures that require time-domain simulations for a large time span in order to take into consideration the slow wave propagation.

In this paper, a space adaptive grid is applied for the analysis of evanescent-mode waveguide bandpass filters [4, 5, 6]. These structures have found many applications in satellite communication systems, as preselectors or in multiplexers, due to several advantages over the conventional coupled resonator filters, such as compactness and wide stopbands. The S-parameters of one specific geometry are calculated and compared to results obtained by the conventional FDTD.

II The MRTD scheme

The 3D-MRTD scheme can be derived by representing the field components as a series of cubic spline Battle-Lemarie scaling and wavelet functions in space-domain and pulse function in time. Applying the Method of Moments to the Maxwell's equations results in the MRTD equations. Generally, the features of the 3D-MRTD algorithm are similar to those of the 2D-MRTD algorithm. Nevertheless, there are some differences as far as it concerns the implementation of the excitation and of the PML absorber.

In order to use a pulse excitation with respect to space at a specific grid point for a 2D geometry and to obtain an excitation identical to that used by FDTD, the pulse is decomposed in terms of scaling and wavelet functions on a square surface around the excitation point. For the 3D-MRTD algorithm, this decomposition takes place in a cubic volume around this point, since the excitation affects the amplitudes of the scaling and the wavelet function in all 3 directions. It has been observed that 4 cells along each direction around the excitation point provide an accurate representation of the source for most cases.

The maximum allowable time step required for the stability of 3D-MRTD algorithms has to contain the effect of all three space discretizations. For a summation stencil of 9 terms per direction and for 0-resolution wavelet expansion it takes the value

$$\Delta t_{max} = \frac{0.37\ c}{\sqrt{1/(\Delta x)^2 + 1/(\Delta y)^2 + 1/(\Delta z)^2}}$$

where c is the velocity of light. For larger stencils, the maximum value of the time step takes lower values.

0-7803-4471-5/98/$10.00 © 1998 IEEE

The size of the stencil affects significantly the dispersion characteristics of the used algorithm. Larger stencil for the summations including scaling functions coefficients improves the phase error performance for medium and high sampling rates (discretization size $\leq \lambda/10$). Increasing the stencil size in summations of wavelet functions coefficients offers a better dispersion performance for lower sampling rates (between $\lambda/2.2$ and $\lambda/5$). In our simulations, the used stencil size has had the value of 9 for a phase error smaller than 1^0 for most discretizations.

The use of the non-localized Battle-Lemarie basis functions causes significant effects. Localized boundary conditions are impossible to be directly implemented, so perfect electric and magnetic boundary conditions are modelled by use of the image principle in a generic way. The implementation of image theory in 3 dimensions is performed automatically for any number of PEC, PMC boundaries.

Due to the nature of the Battle-Lemarie expansion functions, the total field is a summation of the contributions from the non-localized scaling and wavelet functions in 3 directions. For example, the total electric field $E_x(x_o, y_o, z_o, t_o)$ with $(k-1/2)\,\Delta t < t_o < (k+1/2)\,\Delta t$ is calculated

$$E_x(x_o, y_o, z_o, t_o) =$$
$$\sum_{l',m',n'=-l_1}^{l_1} {}_kE^{\phi x}_{l'+1/2,m',n'}\,\phi_{l'+1/2}(x_o)\,\phi_{m'}(y_o)\phi_{n'}(z_o) +$$
$$\sum_i \sum_{l',m',n'=-l_{2,i}}^{l_{2,i}} {}_kE^{\psi_i x}_{l'+1/2,m',n'}\,\phi_{l'+1/2}(x_o)\,\phi_{m'}(y_o)\,\psi_{i,m'}(z_o)$$

where $\phi_m(x) = \phi(\frac{x}{\Delta x} - m)$ and $\psi_{i,m}(x) = \psi_i(\frac{x}{\Delta x} - m)$ represent the Battle-Lemarie scaling and i-resolution wavelet functions respectively. Only wavelets to z-direction have been included for simplicity. For an accuracy of 0.1% the values $l_1 = l_{2,i} = 6$ have been used.

The purpose of a space adaptive grid is to use a coarse mesh and implement a local magnification by the selective use of wavelets. Wavelets are placed only at locations where the EM fields have significant values, creating a space- and time- adaptive dense mesh in regions of strong field variations without adding a significant computational overhead. There are many different ways to take advantage of the capability of the MRTD technique to provide space and time adaptive gridding. All of them rely on the fact that the wavelet values can be thresholded without affecting the accuracy of the algorithm. The simplest way is to threshold the wavelet components to a fraction (usually $\leq 0.5\%$) of the scaling function coefficient at the same cell for each time-step. All components below this threshold are eliminated from the subsequent calculations. This procedure doesn't add any significant overhead in execution time (usually $\leq 12\%$), but it offers only a moderate economy in memory requirements (round $28-35\%$). Comparison of the wavelet values over a specific space window of scaling neighboors (often equal to the stencil size) would offer a more significant economy in memory, but would demand more execution time. Another way of creating a space adaptive grid is to use an absolute threshold. This requires the knowledge of the spatial field distribution in advance, something that makes it inappropriate for simulations of complicated structures. Generally, in 3D cases where both memory and execution requirements are high, the first thresholding algorithm offers an optimized performance.

III Applications of Nonlinear MRTD

Without loss of generality, the space adaptive algorithm used in all simulations presented herein includes one resolution of wavelets only to the z- (longitudinal) direction. For validation purposes, this scheme has been used for the analysis of the testing structure of Figure (1). This filter geometry contains four bilateral E-plane fins in a single WR62 waveguide housing (15.799 mm × 7.899 mm). The thickness of the fins is t=0.9 mm and the gap width is w=3.1mm. The agreement of data obtained from the space adaptive grid for a relative threshold of 0.5% and those obtained by use of mode matching [4] is very good (Figure(2)).

Another evanescent-mode E-plane finned waveguide bandpass filter geometry is shown in Figure(3). A WR90 waveguide (22.86 mm × 10.16 mm) is used at the input and output stages and a rectangular

waveguide with a crossection of 7.06 mm × 6.98 mm is used as the housing of the filter. Geometrical parameters of the filter take the values $l_1 = l_2$ =0.5 mm, l_3 =7.75mm and l_4=0.94mm. The width of the fins is chosen to be equal to the waveguide side length $a = w$ =7.06 mm. The MRTD space adaptive grid is used to optimize the geometry. An 20x20x389 grid is used for the simulations and 85,000 time steps are considered. A Gabor pulse from 10-18 GHz is used as the excitation along a plane at $z = 44$. Front and back waveguides are terminated with 8 PML layers with $R = 10^{-5}$. A relative threshold of 0.5% is employed and offers economy in memory at least by 32%.

In the geometry under study, we have different electrical paths between the input and output ports; one (the main path) is constructed with the coupled $TE_{10} - TE_{10} - TE_{10}$ modes, and the others (the subsidiary paths) are constructed with the coupled $TE_{10} - TE_{m0} - TE_{10}$ modes, where TE_{m0} for $m \geq 1$ express the higher order evanescent modes. These modes play primarily an important role to produce a desired off-passband performance, but it also affects significantly the passband behavior. Therefore, we can not use the conventional synthesis method. The slow velocity of the evanescent waves, require the use of very dense grids of the conventional FDTD algorithm for a large number of time-steps (close to 150,000). For example, a grid of 90x20x778 has been used for 135,000 steps to provide comparable results. On the contrary, space adaptive MRTD algorithms can use coarse grids everywhere except from the areas that the evanescent modes have significant values. Localized use of wavelets in these regions offer the necessary grid magnification. This effect can be observed in Figure(4) that shows the wavelet coefficients amplitude for an arbitrary time step after the pulse has propagated along the whole structure. The results from the optimization (Figures (5)-(7)) show that as the used fins get wider and come closer, the S_{21} gets higher values without affecting the significantly the bandwidth of the filter.

IV Conclusion

A space adaptive 3D algorithm based on Battle-Lemarie scaling and wavelet functions has been applied in the numerical modeling of evanescent-mode waveguide bandpass filters. The S-parameters of one specific geometry are calculated and offer memory savings by a factor of 3-6 per dimension and execution time savings by a factor of 2.5 compared to results obtained by the conventional FDTD.

V Acknowledgments

This work has been funded by ARO.

References

[1] E.Tentzeris, R.Robertson, A.Cangellaris and L.P.B.Katehi, "Space- and Time- Adaptive Gridding Using MRTD", Proc. MTT-S 1997, pp.337-340.

[2] M.Krumpholz, L.P.B.Katehi, "MRTD: New Time Domain Schemes Based on Multiresolution Analysis", IEEE Trans. Microwave Theory Tech., pp. 555-572, 1996.

[3] E.Tentzeris, R.Robertson, M.Krumpholz and L.P.B.Katehi, "Application of the PML Absorber to the MRTD Technique", Proc. AP-S 1996, pp. 634-637.

[4] J.Bornemann and F.Arndt, "Rigorous Design of Evanescent-Mode E-Plane Finned Waveguide Bandpass Filters", Proc. MTT-S 1989, pp. 603-606.

[5] V.Labay and J.Bornemann, "A New Evanescent-Mode Filter for Densely Packaged Waveguide Applications", Proc. MTT-S 1992, pp.901-904.

[6] K.Iguchi, M.Tsuji and H.Shigesawa, "Negative Coupling between TE_{10} and TE_{20} Modes for Use in Evanescent-Mode Bandpass Filters and their Field-Theoretic CAD", Proc. MTT-S 1994, pp. 727-730.

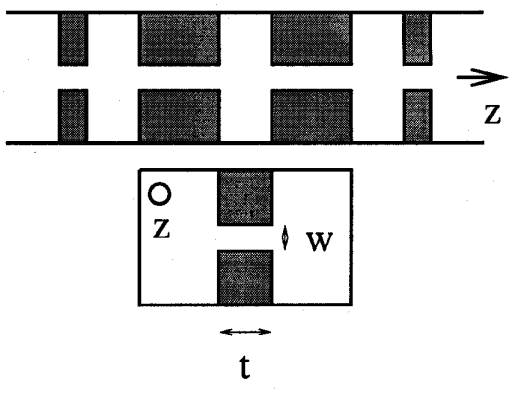

Figure 1: Validation Structure.

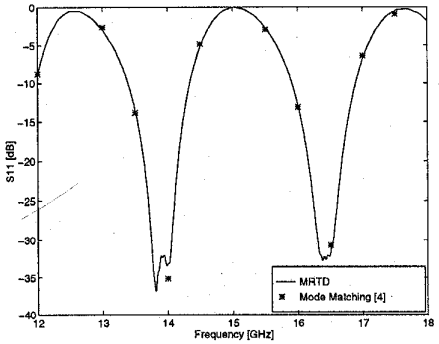

Figure 2: Validation Data.

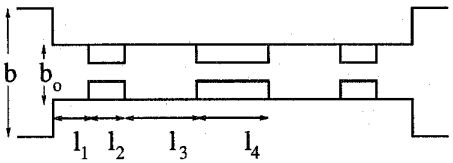

Figure 3: Optimized Filter Geometry.

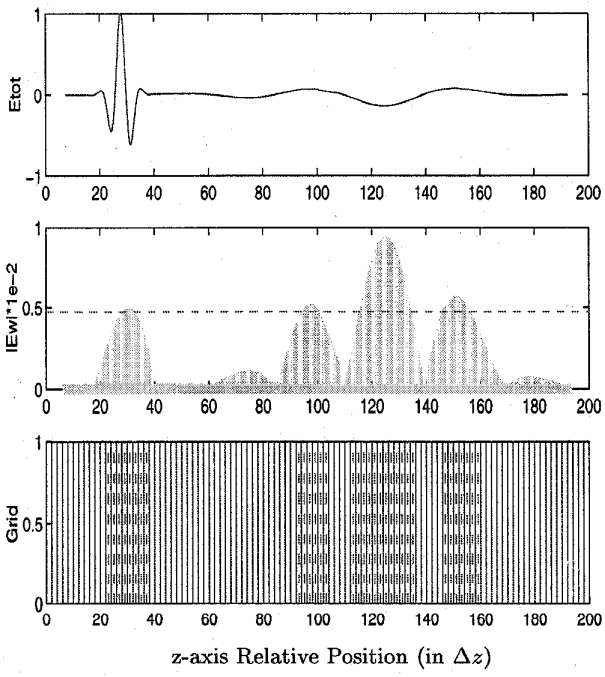

Figure 4: Wavelet Coefficients Spatial Distribution (Δz : cell size to the z-direction).

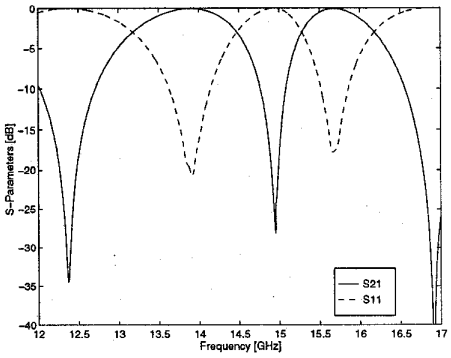

Figure 5: S-Parameters for $l_1 = l_4$ =1.0mm, l_2 =0.5mm, l_3 =6.75mm.

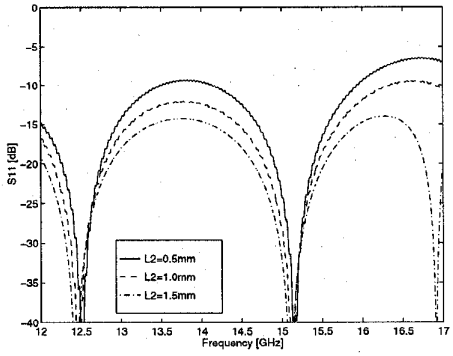

Figure 6: Parametric Variation of S_{21} for l_2.

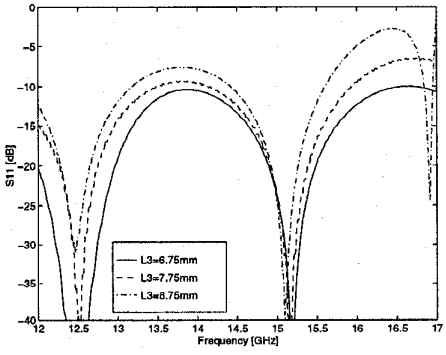

Figure 7: Parametric Variation of S_{21} for l_3.